Analysis and Research on Load Behavior of H-shaped Steel Concrete

Yi Qin *

School of Civil and Transportation Engineering, Beijing University of Civil Engineering and Architecture, Beijing, China

* Corresponding Author Email: 202102020322@stu.bucea.edu.cn

Abstract. Steel-reinforced concrete (SRC) possesses excellent strength and numerous advantages over traditional concrete, making it extensively used in high-rise buildings and large-span bridge structures. This paper commences with the constitutive relationship of steel reinforcement in SRC, the nominal stress-strain conversion, and real stress-strain transformation. It employs Abaqus for nonlinear finite element analysis to study the stress variations in compressed SRC columns subjected to reciprocating loads and examines load-displacement curves. The paper analyzes the hysteresis loops of SRC columns under reciprocating loads, the trends in skeleton curves, energy dissipation, and stiffness degradation. Consequently, it concludes that the variation of compressive stress along the axis of SRC columns is consistent with the change in bearing capacity. Under reciprocating loads, the stress at the lower end of the SRC column is greater than that at the upper end, suggesting the need for reinforcement in the lower portion. The hysteresis loop of SRC columns exhibits a rich characteristic, with increasing energy absorption as displacement increases.

Keywords: SRC Column; finite element analysis; hysteresis loop; stiffness.

1. Introduction

Steel-reinforced concrete (SRC) is a composite structure formed by combining structural steel and plain concrete or reinforced concrete. It effectively resists axial and lateral forces acting on the structure [1]. SRC structures, dating back to the last century, were initially adopted in the US and UK for reinforced concrete technology. The UK later improved SRC column design in the 1960s [2]. China adopted SRC technology relatively later, and it witnessed rapid development in construction projects alongside economic growth in the 1980s [3]. SRC's early origins and its gradual integration into more constructions reflect its development and increasing utilization.

SRC offers numerous advantages, particularly in comparison to regular reinforced concrete, enhancing structural load-bearing capacity. During construction, the steel framework of SRC can serve as a platform, reducing project duration [4]. SRC is also extensively used in high-rise structures and large-span bridges. In China's architectural landscape, many high-rise buildings employ SRC for structural components. Examples include the Jin Mao Tower in Shanghai, which utilizes H-shaped SRC columns, as well as the Senmao Building in Dalian and the Jingguang Building, both employing SRC frameworks [3]. The widespread use of SRC in tall buildings underscores its superior performance.

In building structures, load-bearing columns constitute a vital component, transmitting forces and ensuring building safety by transferring loads to the foundation. Columns mainly endure compression, but in cases of eccentrically loaded columns, tensile forces also arise. Additionally, under seismic or wind loading, columns undergo oscillations. Thus, column fatigue behavior is crucial. Although there has been extensive research on SRC columns globally, spanning several decades and yielding significant results, many aspects still require refinement [5].

This paper follows the construction requirements outlined in the “Technical Specification for Steel Reinforced Concrete Composite Structures” (JGJ 138-2001) to design an SRC column. Subsequently, Abaqus is utilized for numerical simulation, employing the control variable method for analysis [6]. The paper investigates the stress behavior of SRC columns under compression and reciprocating loads

while excluding bonding slip between steel bars and SRC. It also explores the relationship between load and displacement.

2. Finite Element Model of SRC Column

Considering a concrete column as the research subject, a 350×350mm SRC column is designed according to the Code for Design of Concrete Structures (GB50010-2010) [7]. The longitudinal reinforcement ratio of steel bars is 0.85%. H-shaped steel is embedded within the concrete, with 175×175 size H-shaped steel configured based on Hot Rolled H-Shaped Steel and Split T-Shaped Steel (GB/T11263-2017). The material is q345 [8]. The protective layer is 50mm, adhering to the requirement that protective layers exceeding 50mm necessitate effective protection measures, although this model's protective layer is not over 50mm. Therefore, this model does not include steel mesh protection. The concrete strength is C65, modeled using a plastic damage model, with the damage factor set around 0.99 after several experiments, resulting in a well-modeled curve [7]. Specific model parameters can be found in Fig. 1, Table 1, and Table 2.

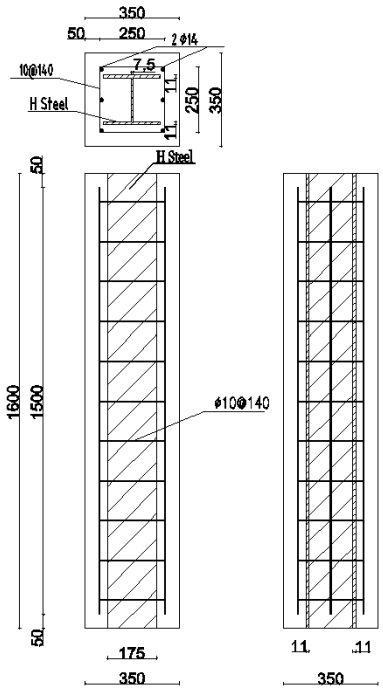


Fig. 1. Reinforcement Layout Diagram of SRC Column.

Table 1. Concrete Material Properties.

Concrete Grade	Density (kg/m³)	Young's Modulus (MPa)	prxy	Dilation Angle	Eccentricity Ratio	f_{b0} / f_{c0}	k	Viscous Coefficient
C65	2400	36500	0.2	35	0.1	1.16	0.667	0.001

Table 2. Steel Reinforcement Material Properties.

Steel Grade	Type	Usage	Young's Modulus (E_s / MPa)	Yield Strength (f_y / MPa)	Ultimate Strength (fu / MPa)
HRB335	B10	Stirrup	200000	335	455
HRB400	C16	Longitudinal Reinforcement	200000	400	540

Steel adopts Reinforcement Constitutive - Bilinear model, and the bilinear model is employed with the following equations:

$$E_2 = 0.01E_1 \quad (1)$$

$$\varepsilon_y = \frac{\sigma_y}{E_1} \tag{2}$$

$$\varepsilon_u = \varepsilon_y + \frac{(\varepsilon_u - \varepsilon_y)}{E_2} \tag{3}$$

Where E_1 is Initial Elastic Modulus, E_2 is Elastic Modulus after Yield, ε_y is Strain after Steel Yield, σ_y is Stress after Steel Yield, and ε_u is Ultimate Strain of Steel. The nominal stress and strain of the section steel is converted into the true stress and strain, and the formula is shown as below [9]:

$$\sigma = \sigma_{com}(1+\varepsilon_{com}) \tag{4}$$

$$\varepsilon = \ln(1+\varepsilon_{com}) \tag{5}$$

Where σ_{com} is Nominal Stress from Experiments and ε_{com} is Nominal Strain from Experiments. The material for H-shaped steel is Q345, and the stress-strain curve is shown in Fig.2 [10]. Fig. 3 shows the configuration diagram of SRC model.

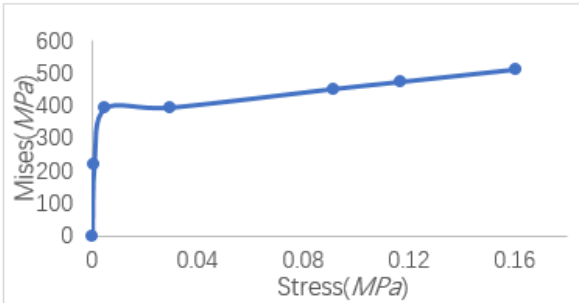


Fig. 2. Q345 Stress-Strain Curve.



Fig. 3. SRC Column Model Configuration.

3. Analysis of Compressive Bearing Capacity of SRC Column

3.1. Model Loading and Boundary Conditions

As shown in Fig. 4, a fixed bottom with a downward force along the y-axis is applied above the concrete axis. The loading is incrementally increased using time-displacement loading in a linear manner, with a maximum vertical displacement of 15mm. Fig. 5 shows the displacement time loading curve.

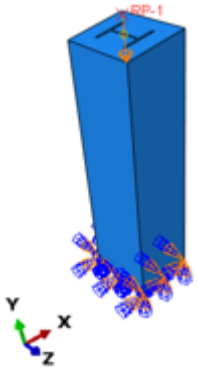


Fig. 4. Boundary Conditions.

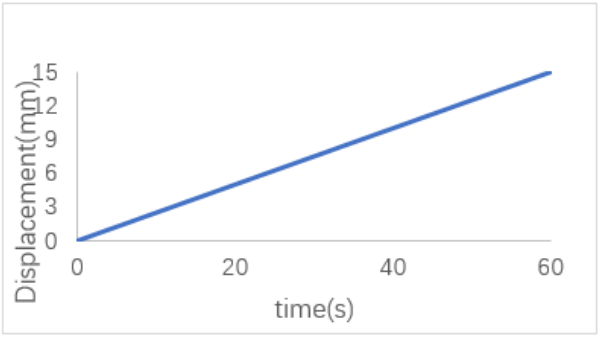


Fig. 5. Time-Displacement Loading Curve.

3.2. Analysis of Compressive Results

The surface stress of the SRC concrete is generally small, mostly around 3.937MPa. Conversely, the steel surface experiences higher stress, around 108.1MPa, indicating substantial force on the steel surface. To study stress variations in the steel, the upper center of the steel is selected for analysis (as shown in Fig. 6). As seen in the results in Fig. 7, stress initially increases and then decreases over time, reaching a peak stress of 213.653MPa at around 12.14 seconds, followed by a decline.

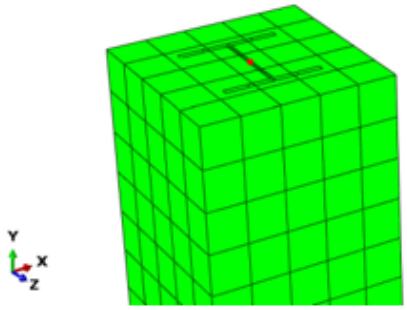


Fig. 6. Illustration of SRC Column Top.

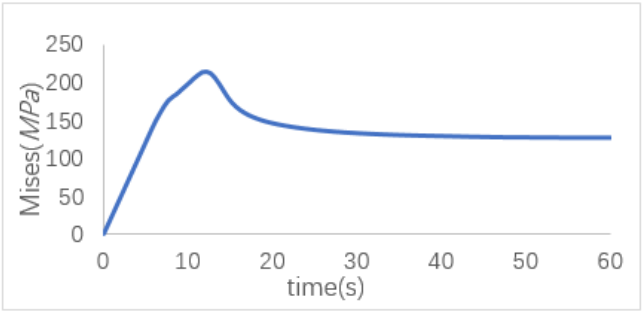


Fig. 7. Stress-Time Curve at H-Shaped Steel Vertex.

From Fig. 8, the load-displacement curve shows that under compression, the SRC column's load and displacement exhibit a linear relationship. The load reaches a maximum of 7470KN at a displacement of 3.03mm. Subsequently, the load decreases, indicating damage to the SRC column. With further displacement increase, the load steadily declines, eventually reaching its stability.

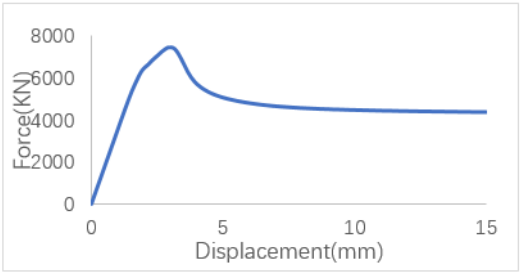


Fig. 8. Compression Load-Displacement Curve for SRC Column.

4. Analysis of SRC Column Under Reciprocating Loads

4.1. Reciprocating Load Loading Curve

Axial compression is applied along the y-axis, and horizontal forces are applied along the x-axis to the SRC column. The z-axis movement of the SRC column is restricted, as well as rotation about the x and y axes. After applying axial force of 750KN, reciprocating loads are applied. Displacement loading is shown in Fig. 9, and the model loading is depicted in Fig. 10.

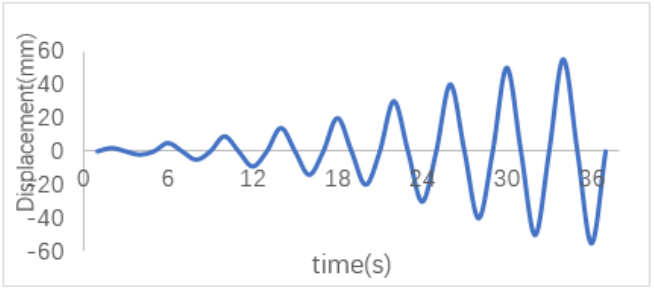


Fig. 9. Displacement-Time Loading Diagram.

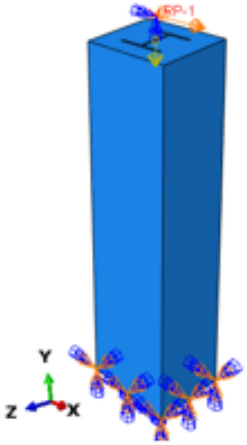


Fig. 10. Model Loading Schematic.

4.2. Stress Analysis of Reciprocating Load Results

After reciprocating loads, the surface stress distribution of the SRC concrete is uniform, with relatively low stress. To observe the internal structure, the outer concrete layer is removed using Boolean operations. The upper-side stress values of the steel and reinforcement are around 4.539MPa, while the lower-side stress is higher. The steel's lower region, near the bottom flange area, experiences stress reaching 540MPa. Generally, the lower part bears more stress than the upper. Two units at the lower end of the steel are analyzed for comparison (as shown in Fig. 11). As depicted in Fig. 12, within 0-10s, stress values are relatively similar, but after 10 seconds, the units closer to the bottom experience higher stress, peaking at approximately 400MPa. Stress fluctuates with reciprocating load action. Consequently, under reciprocating loads, the bottom of the column experiences higher stress than the top, suggesting that failure is more likely to occur near the bottom. The selected units are shown in Fig. 11.

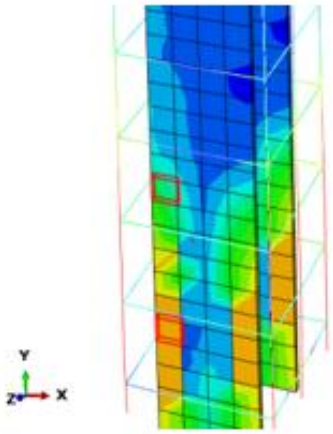
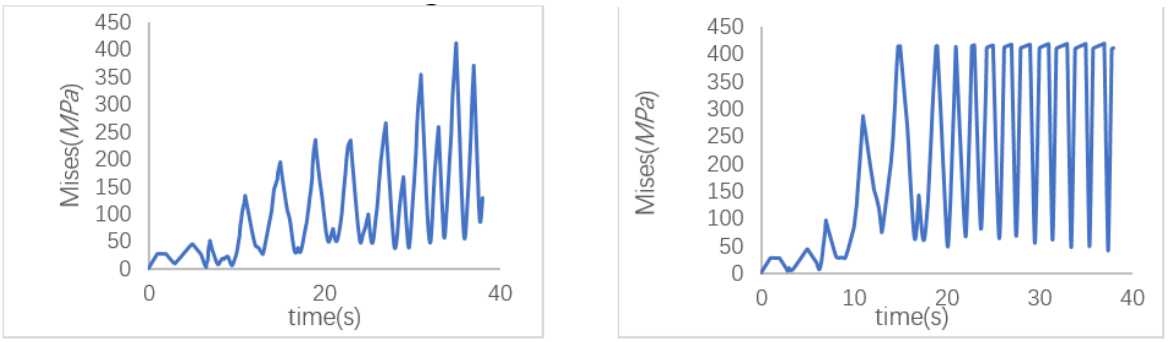


Fig. 11. Selected Units Diagram.



(a) Upper Unit of H-Shaped Steel **(b)** Lower Unit of H-Shaped Steel

Fig. 12. Time-Stress Relationship Diagram.

4.3. Hysteresis Loop Analysis

Fig. 13 illustrates the displacement-load curve for the SRC column. As the x-axis displacement increases, the bearing capacity of the SRC column gradually increases and then decreases. The maximum positive bearing capacity is 152KN, corresponding to a displacement of 6.44mm, while the maximum negative bearing capacity is 159KN, corresponding to a displacement of 8.82mm. Overall, the decline in bearing capacity is relatively gradual, indicating that the steel-reinforced concrete column maintains a certain load-bearing capacity even under significant displacement, thereby avoiding sudden failure.

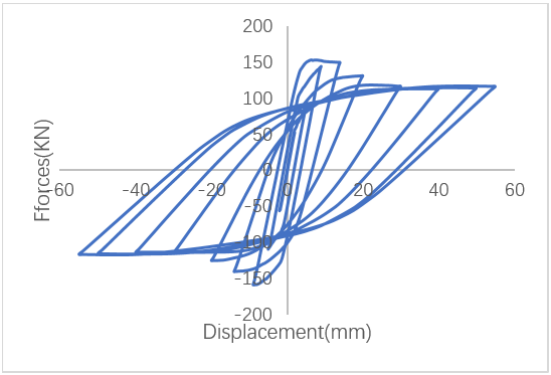


Fig. 13. Displacement-Load Curve of SRC Column.

4.4. Skeleton Curve

The skeleton curve represents the connection of peak values of each hysteresis loop, reflecting the restoration characteristics of the steel-reinforced concrete column under cyclic loading. From the skeleton curve, there are rising and falling segments. Initially, during the elastic phase, the stiffness is relatively high. However, with increasing displacement, the stiffness decreases until reaching the peak value, at which point the bearing capacity is maximal. As displacement continues to increase, the bearing capacity decreases. Fig. 14 shows the skeleton curve.

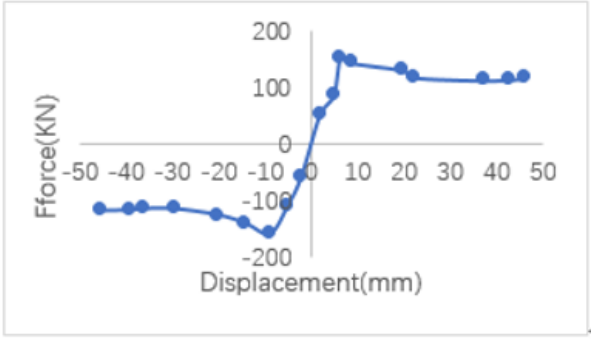


Fig. 14. Skeleton Curve.

4.5. Cumulative Hysteresis Curve and Energy Dissipation

Energy dissipation can be determined from the area enclosed by each hysteresis loop. Cumulative hysteresis energy is the sum of these areas [11]. Energy dissipation represents a structure's ability to absorb energy through its plastic deformation, making it a significant parameter for structural evaluation [12]. The formula for calculating cumulative energy dissipation is presented below:

$$E_H = \sum_{i=1}^{n} E_{Di} \tag{6}$$

$$E_{Di} = \int F d\Delta \tag{7}$$

Where n is Number of loading cycles, F is Horizontal load during cyclic loading (KN), Δ is Horizontal displacement (mm), EDi is Hysteresis energy dissipation at level i (KN·mm), and E_H is Cumulative hysteresis energy dissipation under cyclic loading (KN·mm).

In this simulation, a total of nine hysteresis loops were obtained, yielding a total energy of 46467 KN·mm. The energy dissipation for each loop is shown in Table 3. Fig. 15 presents the cumulative energy dissipation with increasing displacement. As displacement increases, the energy dissipation for each loop also increases, with the growth rate accelerating. The final two loops account for approximately 50% of the total energy dissipation.

Table 3. Hysteresis Energy Dissipation Values.

Displacement (mm)	Hysteresis Energy Dissipation (KN·mm)	Energy Dissipation Ratio (%)
2	13.4272	0.0288
5	398.3480	0.8572
9	1527.9983	3.2883
14	3077.78025	6.6235
20	3497.9750	7.5278
30	5928.1390	12.7576
40	8462.1239	18.2109
50	11283.0032	24.2819
55	12278.4909	26.4239

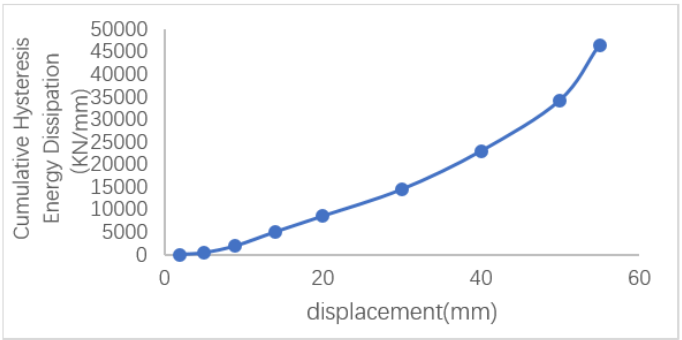


Fig. 15. Cumulative Hysteresis Energy Dissipation Curve.

4.6. Stiffness Variation

From the skeleton curve, it can be observed that stiffness varies continuously with displacement. The initial stiffness is the highest, and as displacement increases, the stiffness gradually decreases. This phenomenon is referred to as stiffness degradation [13]. The secant stiffness is the slope of the line connecting positive and negative displacement load curves. In order to better observe its stiffness variation, the ratio of secant stiffness to initial stiffness is used to reflect its stiffness characteristics. The formula is as follows:

$$K_{si} = \frac{|+F_i| + |-F_i|}{|+\Delta_i| + |-\Delta_i|} \tag{8}$$

$$\eta = \frac{K_S}{K_0} \tag{9}$$

From Figure 16, it is observed that the degradation coefficient of the SRC column decreases rapidly as displacement increases under cyclic loading. However, with further displacement increase, the rate of degradation slows down, indicating that the SRC column enters the plastic phase.

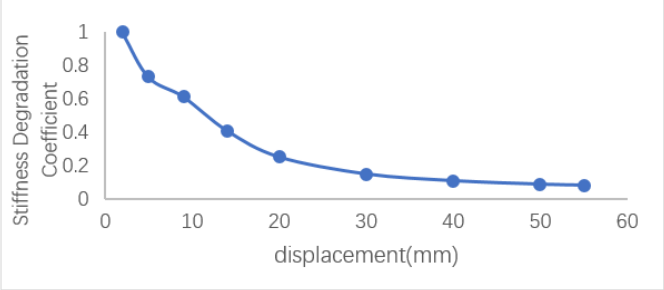


Fig. 16. Stiffness Degradation Coefficient.

5. Conclusion

This study primarily investigated the stress distribution and load-displacement relationship of SRC columns under axial compression and cyclic loading, as well as their energy dissipation characteristics. The following conclusions are drawn:

(1) The stress distribution in the SRC column's axial compression is closely related to the presence of concrete damage. After the bearing capacity of the SRC column decreases, its stress also decreases. Concrete damage occurs when the axial compression of the SRC column exceeds 3mm, leading to a reduction in bearing capacity. However, the decline in bearing capacity is not substantial.

(2) Under cyclic loading, the lower end of the SRC column experiences higher stress than the upper end. Therefore, in structures subject to significant cyclic loading, reinforcing the lower portion of the column may be necessary.

(3) Based on the skeleton curve, the stiffness of the SRC column decreases rapidly with increasing displacement, but the degradation of stiffness slows down as the degradation coefficient approaches 0.2, indicating the onset of plastic deformation.

(4) The hysteresis curve of the SRC column is well-rounded, and as displacement increases, the energy absorbed also increases significantly, resulting in higher energy dissipation capacity.

References

[1] A. Gautham, Dipti Ranjan Sahoo. Behavior of steel-reinforced composite concrete columns under combined axial and lateral loading. Journey of Building Engineering, 2021, 39, 102305.

[2] Wang Lianguang, Liu Zhiyang. Progress in the application and research of steel-reinforced concrete structures at home and abroad. Journal of Northeastern University, 1995, (03): 238-242.

[3] Yu Qingrong, Jiang Weishan, GAO Yongfu, et al. Development of steel-reinforced concrete structures in China. Tianjin Construction Science and Technology, 2003 (05): 8-13.

[4] Tang Yong. Overview of the development status of steel-reinforced concrete structures. China Construction, 2020 (8): 202-203.

[5] Sheng Weizhong, Shao Yongjian, Li Guojian. Study on the influence of ABAQUS constitutive curve truncation on the torsional behavior of SRC columns.

[6] JGJ 138-2001, Technical specification for steel-reinforced concrete composite structures.

[7] GB 50010-2010, Code for design of concrete structures.
[8] GB/T 11263-2017, Hot-rolled H-shaped steel and split T-shaped steel.
[9] Zhuang Zhuo. Finite Element Analysis and Application Based on ABAQUS. Tsinghua University Press, 2009-1-1.
[10] Sun Dechang, Zhang Hailong, Yan Fengzuo, et al. Static test and numerical analysis of box-shaped steel piers with embedded energy-absorbing steel plates. Advances in Steel Structures: 1-10.
[11] Fujino Y, Hashimoto S, Abe M. Damage analysis of Hanshin Expressway viaducts during 1995 Kobe earthquake. I: Residual inclination of reinforced concrete piers Journal of Bridge Engineering, 2005, 10(1): 45-53.
[12] Wu Wanyan. Seismic research on self-compacting concrete bridge piers with mixed fibers. Suzhou University of Science and Technology, 2022.000155.
[13] Takeda T, Sozen M A, Nielsen N N. Reinforced concrete response to simulated earthquakes. Journal of the structural division, 1970, 96(12): 2557-2573.